Biomaterials and Biosystems 8 (2022) 100066

Contents lists available at ScienceDirect

Biomaterials and Biosystems

journal homepage: www.elsevier.com/locate/bbiosy

Evaluation of a co-culture of rapidly isolated chondrocytes and stem cells seeded on tri-layered collagen-based scaffolds in a caprine osteochondral defect model

Tanya J. Levingstone[a,b,c,d,e,1], Eamon J. Sheehy[d,e,f,1], Conor J. Moran[d,e], Gráinne M. Cunniffe[e,g,h], Pedro J. Diaz Payno[e,g], Robert T. Brady[d,e], Henrique V. Almeida[e,g,i,j], Simon F. Carroll[e,g], John M. O'Byrne[d,k], Daniel J. Kelly[e,g], Pieter AJ. Brama[l], Fergal J. O' Brien[d,e,f,*]

[a] School of Mechanical and Manufacturing Engineering, Dublin City University, Dublin 9, Ireland
[b] Centre for Medical Engineering Research (MEDeng), Dublin City University, Dublin 9, Ireland
[c] Advanced Processing Technology Research Centre, Dublin City University, Dublin 9, Ireland
[d] Tissue Engineering Research Group, Department of Anatomy and Regenerative Medicine, Royal College of Surgeons in Ireland (RCSI), 123St. Stephen's Green, Dublin 2, Ireland
[e] Trinity Centre for Biomedical Engineering (TCBE), Trinity Biomedical Sciences Institute, Trinity College Dublin (TCD), Dublin 2, Ireland
[f] Advanced Materials and Bioengineering Research (AMBER) Centre, RCSI & TCD, Ireland
[g] Department of Mechanical, Manufacturing and Biomedical Engineering, School of Engineering, Trinity College Dublin, Ireland
[h] National Spinal Injuries Unit, Mater Misericordiae University Hospital, Dublin, Ireland
[i] iBET, Instituto de Biologia Experimental e Tecnológica, 2781-901 Oeiras, Portugal
[j] Instituto de Tecnologia Química e Biológica António Xavier, Universidade Nova de Lisboa, 2780-157 Oeiras, Portugal
[k] Cappagh National Orthopaedic Hospital, Finglas, Dublin 11, Ireland
[l] Section Veterinary Clinical Sciences, School of Veterinary Medicine, University College Dublin, Dublin 4, Ireland

ARTICLE INFO

Keywords:
Tissue engineering
Collagen
In vivo
Osteochondral
Cartilage
Caprine model

ABSTRACT

Cartilage has poor regenerative capacity and thus damage to the joint surfaces presents a major clinical challenge. Recent research has focussed on the development of tissue-engineered and cell-based approaches for the treatment of cartilage and osteochondral injuries, with current clinically available cell-based approaches including autologous chondrocyte implantation and matrix-assisted autologous chondrocyte implantation. However, these approaches have significant disadvantages due to the requirement for a two-stage surgical procedure and an in vitro chondrocyte expansion phase which increases logistical challenges, hospital times and costs. In this study, we hypothesized that seeding biomimetic tri-layered scaffolds, with proven regenerative potential, with chondrocyte/infrapatellar fat pad stromal cell co-cultures would improve their regenerative capacity compared to scaffolds implanted cell-free. Rapid cell isolation techniques, without the requirement for long term in vitro culture, were utilised to achieve co-cultures of chondrocytes and stromal cells and thus overcome the limitations of existing cell-based techniques. Cell-free and cell-seeded scaffolds were implanted in osteochondral defects, created within the femoral condyle and trochlear ridge, in a translational large animal goat model. While analysis showed trends towards delayed subchondral bone healing in the cell-seeded scaffold group, by the 12 month timepoint the cell-free and cell-seeded groups yield cartilage and bone tissue with comparable quality and quantity. The results of the study reinforce the potential of the biomimetic tri-layered scaffold to repair joint defects but failed to demonstrate a clear benefit from the addition of the CC/FPMSC co-culture to this scaffold. Taking into consideration the additional cost and complexity associated with the cell-seeded scaffold approach, this study demonstrates that the treatment of osteochondral defects using cell-free tri-layered scaffolds may represent a more prudent clinical approach.

* Corresponding author at: Department of Anatomy and Regenerative Medicine, Royal College of Surgeons in Ireland, 123St. Stephen's Green, Ireland.
[1] The first two authors contributed equally to this manuscript

https://doi.org/10.1016/j.bbiosy.2022.100066
Received 4 July 2022; Received in revised form 5 October 2022; Accepted 7 October 2022

Introduction

Articular cartilage damage is a growing problem worldwide with arthritis affecting 9.6% of men and 18% of women over the age of 60 in Europe [1]. An intact smooth cartilage layer is vital for pain-free movement of synovial joints, however, the ability of the articular cartilage to self-repair when damaged is limited. Small cartilage lesions are typically addressed surgically through marrow stimulation techniques such as microfracture or drilling [2], although the newly generated tissue has been reported to be fibro- as opposed to hyaline cartilage and thus may not result in long-lasting repair [3,4]. Larger cartilage lesions are often treated using approaches such as osteochondral autograft transplantation (OAT), whereby an osteochondral plug (or plugs in the case of mosaicplasty) is harvested from a non-load bearing part of the joint and implanted into the defect site [5,6]. This approach, however, results in donor site morbidity [7] and there is also a limitation on the quantity and quality of tissue available for harvest. These drawbacks have led to increased interest in novel, alternative strategies for promoting cartilage regeneration.

Cell-based approaches, such as autologous chondrocyte implantation (ACI) and matrix-assisted autologous chondrocyte implantation (MACI), have shown some promise for cartilage repair applications [8,9]. These procedures represent two-stage cell-based therapies, whereby chondrocytes (CCs), isolated from cartilage biopsies harvested in stage one of the procedure, are expanded prior to implantation in stage two [10]. Although these techniques have been used in a clinical setting for numerous years, they have a number of associated limitations. The expansion of cells harvested in stage one of the procedure, for example, typically lasts for 3–5 weeks [11], resulting in high costs [12]. CCs have also been shown to lose their chondrogenic phenotype when isolated from their 3D environment and expanded in vitro, leading to de-differentiation down a fibrogenic pathway [13–15]. Furthermore, the proliferative capacity of the harvested CCs does not suffice for the treatment of large defects [14]. In addition, the clinical benefit of these procedures over procedures such as microfracture remains unclear. Hong-Chul et al. compared ACI, OAT and microfracture in 30 knees with arthroscopy at 1 year showing that 80% had excellent or good results after microfracture, 82% after OAT, and 80% after ACI [16]. Follow-up at 3 years showed no differences in functional scores and postoperative MRI grades amongst the groups. Furthermore, a recent systematic review by Gou et al. comparing the results of 12 randomised control trials and a total of 659 patients showed that although patients treated with ACI may report some benefits relating to activities of daily living, and quality of life compared with patients treated with microfracture, no significant improvement in International Knee Documentation Committee or Lysholm scores, or overall Knee Injury and Osteoarthritis Outcome Score measures was reported between patients in the ACI and microfracture groups at 1 to 5 years of follow-up [17]. Thus, because of the cost and complexities associated with cell-based approaches for cartilage repair applications, understanding their potential clinical benefits over more cost-effective, off-the-shelf treatment methods remains an important question in orthopaedic medicine.

A biomimetic tri-layered collagen-based scaffold has recently been developed in our lab as a promising off-the-shelf cell-free scaffold for the treatment of osteochondral lesions [18–21]. The highly porous nature of this scaffold allows for the infiltration of host bone marrow stromal cells when implanted into osteochondral defects and directs these cells to form the required tissue type within each layer of the defect [21]. In addition, the potential of this scaffold to direct the repair of osteochondral tissues has previously been demonstrated in a small animal (rabbit) model [20], and in a large animal (goat) study where the cell-free tri-layered scaffold was shown to promote greater levels of cartilage and bone regeneration when compared to empty defects and a leading commercial comparator [21]. Additionally, this scaffold has shown success in the treatment of osteochondritis dissecans in an equine clinical case study [19].

In this study, we hypothesised that seeding the tri-layered scaffolds with a chondrogenic cell source would result in an enhanced therapeutic response, leading to more rapid repair and potentially enabling the treatment of larger defects. Various cell-seeding approaches have shown potential in cartilage repair applications. Due to the limitations associated with autologous CCs the use of alternative cell sources such as bone marrow mesenchymal stem cells (MSCs), infrapatellar fat pad MSCs (FPMSCs), nasal CCs, human embryonic stem cells, induced pluripotent stem cells and adipose-derived stem cells have been extensively explored [22–32]. FPMSCs, either used alone or as a co-culture with CCs, have shown particular promise in achieving high levels of cartilage matrix deposition in vitro and a higher capacity for chondrogenic differentiation than MSCs from other sources [7,11]. FPMSCs also have other associated advantages as biopsy of these cells can be easily achieved during diagnostic arthroscopy without causing morbidity to the patient [31]. In addition, they have been shown to retain their chondrogenic potential, even in the diseased state which is clinically important for patients who may present with osteochondral defects that already show evidence of osteoarthritic changes [24]. Furthermore, novel techniques have recently been developed which allow for the rapid isolation of stromal cells from the infrapatellar fat pad [33]. This raises the possibility of circumventing the costly in vitro expansion phase associated with ACI by utilizing a rapid cell isolation procedure to obtain a clinically relevant number of cells from tissue biopsies taken while a patient is in the theatre. Previous research within our group demonstrated that seeding scaffolds with a co-culture of FPMSCs and CCs, specifically, FPMSC:CC in a 3:1 ratio, resulted in higher levels of chondrogenesis in vitro compared to either CCs or FPMSCs alone, demonstrating a synergistic effect between the two cell types [34]. Building on this evidence base, herein we explore the benefit of a biomimetic tri-layered collagen-based scaffold seeded with a co-culture of FPMSCs and CCs as a framework for future cell-based tissue engineering approaches. These cell-seeded scaffolds were implanted into osteochondral defects created in the femoral condyles and trochlear ridges of goats and compared to cell-free scaffolds that have been previously shown to promote osteochondral regeneration in the same model. Repair of the osteochondral tissues was assessed macroscopically, histologically, and radiologically at 3, 6 months and 12 months in both defect sites.

Materials and methods

Fabrication of tri-layered scaffolds

Tri-layered scaffolds were fabricated using a unique iterative layering fabrication method developed in our lab [18] (Supplementary Fig. S1). Briefly, this process involved fabrication of the bone layer by blending type I collagen (Col1) [0.5% (w/v), Collagen Matrix Inc., NJ, USA] with hydroxyapatite (HA) [1% (w/v) Plasma Biotal, UK] at 4 °C for 4 h to produce a Col1HA slurry, prior to freeze-drying (VirTis Ultra Super XL-70, Biopharma, UK) in a stainless steel tray (60 mm x 60 mm internal diameter) at a freezing rate of 1 °C/min to a final freezing temperature of −40 °C [35]. Following freeze-drying, the scaffold was cross-linked using 1-ethyl-3-(3-dimethylaminopropyl) carbodiimide (EDAC)/N-hydroxysuccinimide (NHS) (Sigma–Aldrich, Arklow, Ireland) at a concentration of 6 mM EDAC g^{-1} of collagen, and a 5:2 M ratio of EDAC:NHS for 2 h at room temperature [36]. The intermediate layer slurry, consisting of Col1 [0.5% (w/v)], and hyaluronic acid sodium salt derived from streptococcus equi. (HyA) [0.05% (w/v), Contipro, Czech Republic] was then added on top of the hydrated bone layer scaffold with freeze-drying repeated as before. Finally, the cartilage layer slurry, consisting of Col1 [0.25% (w/v)], type II collagen (Col2) [0.25% (w/v) porcine type 2 collagen, Symatase, France] and HyA [0.05% (w/v], was added and the process of freeze-drying was repeated as described previously, incorporating prolonged freezing and drying steps to ensure optimal freeze-drying of the tri-layered scaffold sheet. Scaffolds were dehydrothermally (DHT) cross-linked at 105 °C and a pressure of 50

mTorr for 24 h (VC-20 vacuum oven, Salvislab, Switzerland), prior to EDAC cross-linked again under sterile conditions as described previously and drying in the freeze-dryer. Cylindrical scaffold plugs were cut to a diameter of 7 mm and a depth of 6 mm using a biopsy punch in order to provide a secure press-fit on implantation. Following fabrication, the scaffolds were double packaged and sterilised by gamma irradiation using the VD_{max} 25 kGy method by Synergy Healthcare, Tullamore.

Study design

In vivo assessment was carried out in a bi-lateral goat stifle joint model under ethical approval (University College Dublin – AREC-P-12–71) and an animal licence granted by the Irish Government Department of Health (B100/4517). The study complied with the EU Directive 2010/63/EU for animal experiments. Skeletally mature female goats (2–3 years old) were used in the study, with tissue repair assessed 3, 6 and 12 months post-implantation. N-numbers were based on power analysis to provide an $n \geq 6$ per experimental group. Surgeries were carried out bilaterally with two defect sites created per stifle joint, one on the lateral trochlear ridge and the other on the medial femoral condyle. Each joint was assigned to either the cell-free or cell-seeded scaffold group with both sites within the same joint receiving the same treatment. This resulted in a requirement for eight animals per timepoint.

Surgical procedure and scaffold implantation in caprine stifles

Prior to surgery food but not water was withheld for 12 h. Preoperative sedation was provided by an intravenous injection of diazepam (0.4 mg kg^{-1}; Diazemuls®; Accord Healthcare; UK). Anaesthesia was then induced using propofol (Propofol-Lipuro 1%; B. Braun Medical Inc., EU). The larynx was then sprayed with lidocaine (approximately 2 mL per goat; Lidocaine hydrochloride 2%, B. Braun Medical Inc, EU), and the trachea was intubated using a cuffed endotracheal tube. A lumbosacral epidural block was performed with the goat in sternal recumbency. A combination of lidocaine (2 mg kg^{-1}) and morphine (0.1 mg kg^{-1}; Morphine sulphate; Mercury Pharmaceuticals; Ireland) was administered using a 30–50 mm, 20-gauge spinal needle. The goats were positioned in dorsal recumbency for surgery. Anaesthesia was maintained with isoflurane (Vetflurane; Virbac Animal Health, UK) delivered in 100% oxygen via a circle breathing system and mechanical ventilation with a volume controlled ventilator (Carestation CS650 anesthesia Delivery System; GE Healthcare, Ireland). All goats received analgesia with carprofen IV (1.4 mg kg^{-1}; Rimadyl; Pfizer; Ireland); and morphine IV (0.2 mg kg^{-1}; Morphine sulphate; Mercury Pharmaceuticals, Ireland) 90 min after the epidural block. Intravenous fluid therapy (Lactated Ringer's Solution, Vetivex® 11; Braun, Germany) was infused during anaesthesia through the cephalic vein, to deliver approximately 10 mL kg^{-1} h^{-1}. Adequacy of anaesthesia was monitored continuously and recorded every five minutes by assessing the following: heart rate, electrocardiogram and direct arterial blood pressure (systolic, diastolic and mean); respiratory rate, end-tidal CO_2 (F_E´CO_2) and end-tidal isoflurane (F_E´ISO); and haemoglobin oxygen saturation (SpO_2) and temperature using a multiparameter monitor (Carescape B450 Monitor; GE Healthcare, Ireland). The vaporiser setting was adjusted to maintain an F_E´ISOpost surgery of 1.2–1.3%. SpO_2 was measured with a pulse oximeter applied to the tongue or wattles. Rectal temperature was measured before the procedure and during recovery. A warm mattress was applied to maintain normothermia (AniMat, ManoMedical, Taden, France).

A lateral parapatellar mini-arthrotomy was performed on each hind leg by creating a longitudinal incision lateral to the patellar ligament and extending upwards along the lateral border of the patella as described earlier [21]. The joint capsule was opened, and the patella dislocated medially. Approximately $\frac{1}{4}$ of the fat pad present was harvested (roughly 1 g of tissue) and stored in sterile PBS (Sigma-Aldrich, Ireland) at 4 °C. The medial condyle was exposed by flexion and internal rotation of the stifle joint. A 6 mm biopsy punch was used to position two defects on the chondral surface on the medial femoral condyle and the lateral trochlear ridge and cartilage was harvested using a fresh scalpel blade and a sharp curette. The cartilage tissue was stored in sterile PBS (Sigma-Aldrich, Ireland) at 4 °C. The defects were then drilled using a standard 6 mm drill bit in a custom-made drill guide with a 6 mm stop, followed by a flat-bottomed drill bit in a similar guide to create 6 mm x 6 mm cylindrical flat-bottomed critically sized defects. Each joint was then assigned to one of two groups. 1) Cell-free tri-layered scaffold or 2) Cell-seeded tri-layered scaffold with an n of at least 6 used for each group. Scaffolds, 7 mm in diameter x 6 mm in depth, were then implanted into the defects in order to achieve press-fit fixation. The scaffold position was checked, and the surface was palpated to ensure it was flush with the native cartilage tissue [37]. The patella was then relocated, and the capsule, subcutis and skin layers were closed. A stent was sutured in situ over the wound to protect the healing wound.

The goats were allowed to mobilise immediately postoperatively. They were kept in a small (3 m x 3 m) high-sided (2 m) pen for the first 2–4 weeks to limit ambulation and monitored closely. Each goat received a 5-day course of antibiotics intramuscularly (8.75 mg/kg Noroclav, Amoxicillin Trihydrate 140 mg/ml and Potassium Clavulanate 35 mg/ml) Norbrook UK) and non-steroidal anti-inflammatory analgesic (1.4 mg/kg Carprieve (Carprofen) Norbrook, UK) twice daily for the first three days and as required thereafter based on gait and signs of discomfort. The stent was removed after 3 days followed by skin suture removal on day 10 post surgery.

Cell isolation and seeding

While it is envisioned that this approach would be applied clinically using the patient's own cells, the lack of culture facilities at the surgical facility necessitated the use of allogeneic, rather than autologous cells. On the day prior to the 1st surgical procedure, cartilage and fat pad tissue biopsies were taken from a donor goat, the cells were isolated overnight in an off-site facility (TCBE) and seeded on scaffolds for implantation on day 1. Following this, the cells harvested from biopsies taken during the surgical procedures were isolated overnight and seeded on scaffolds for implantation the following day. Numerous studies have reported the use of allogenic chondral transplants in clinical practice [38,39]. This is possible without the risk of immunogenic response due to the immunoprivileged nature of articular cartilage and its avascular nature. The cartilage and fat pad biopsies harvested during the surgical procedure were transported to TCBE under sterile conditions. CCs and FPMSCs were isolated using novel rapid-isolation techniques previously developed in our lab [33,40,41]. Briefly, CCs were harvested by slicing the cartilage into pieces less than 1 mm in size, and rinsing with antibiotic supplemented PBS, and placing in sterile collagenase solution [(Worthington, LS004176 Collagenase Type CLS-2), 8 ml/g cartilage] in a tube rotator (Stuart, UK) for 2 h at 37 °C. The tissue was filtered (40 μm cell strainer) and collected cartilage particles were crushed, added to fresh collagenase solution, rotated for a further one hour (37 °C) and then filtered again (40 μm cell strainer). The media was then mixed with an equal volume of stopping medium [Gibco DMEM + GlutaMAX (61,965, Gibco) + 10% FBS (Foetal Bovine Serum, (Labtech, UK))] prior to centrifuging. The pellet was collected and re-suspended in standard expansion medium [Gibco DMEM + GlutaMAX (61,965, Gibco) + 10% FBS + 10 ml (100 U/ml penicillin G and 100 μg/ml streptomycin sulphate)], and live cells were counted using a trypan blue exclusion test.

For isolation of the FPMSCs, the infrapatellar fat pad tissue was minced, added to collagenase solution (750 U/ml, 4 ml/g of tissue) and rotated in a tube rotator at 37 °C for 3–4 h. Two volumes of stopping medium were added to the tissue collagenase mixture and the solution was sieved (150 μm sieve) prior to centrifuging. The floating fat fraction containing the adipocytes was aspirated off and discarded and the pellet resuspended in fresh standard expansion media and filtered (40 μm cell strainer). Further media was added, the suspension, centrifuged and

the pellet resuspended in fresh media before counting using trypan blue exclusion.

Freshly isolated FPMSCs and CCs were then suspended at a 3:1 ratio of FPMSCs to CCs and seeded onto the cartilage surface of the tri-layered scaffolds using a dropwise technique at a seeding density of 500,000 cells/scaffold and stored in an incubator at 37 °C and 5% CO_2 overnight [34]. This cell seeding approach was based on previous work within our group which demonstrated the benefits of FPMSC:CC co-cultures in promoting chondrogenesis in vitro [34,42]. This study compared scaffolds seeded with chondrocytes and FPMSCs at low and high densities and a co-culture of FPMSCs and CCs at a ratio of 3:1 of FPMSC to CCs. The results demonstrated that the co-culture of FPMSCs and CCs represents the optimal seeding approach, with a 7.8-fold increase in the sGAG production observed in this group compared to seeding with chondrocytes alone. The seeding density of 500,000 cells/scaffold or 12.99×10^6 cells/cm^3, mimics the density of chondrocytes present in normal cartilage tissue while also reflecting the seeding densities currently used clinically in cartilage repair procedures [43,44]. On the morning of surgery, the seeded scaffolds were transported to the surgical facility under sterile conditions and stored in an incubator at 37 °C and 5% CO_2 prior to implantation.

Macroscopic assessment of the level of repair at defect sites

Post euthanasia at 3, 6 and 12 month timepoints, the joints were opened and the defect site and surrounding joint tissues were examined. Synovial fluid was aspirated and inspected. The quality of repair and regeneration within the defect site was assessed using the International Cartilage Repair Society (ICRS) macroscopic evaluation tool (Table S1). This tool rates cartilage repair tissue as Grade IV (severely abnormal), Grade III (abnormal), Grade II (nearly normal) or Grade I (normal) based on the degree of defect repair, degree of integration and macroscopic appearance. Assessors were blinded to the treatment groups until after the macroscopic scoring had been completed. Osteochondral segments containing the defect sites surrounding by a margin of approximately 5 mm were subsequently resected, stored in sterile saline and fixed in 10% formalin for 2–3 days prior to further analysis.

Histological and immunohistochemical assessment of the level of repair at defect sites

Specimens were decalcified (Decalcifying Solution-Lite, Sigma-Aldrich, Arklow, Ireland) and sectioned longitudinally prior to processing using an automated tissue processor (ASP300, Leica, Germany), embedding in paraffin wax blocks and sectioning to a thickness of 10 μm. Sections were stained histologically using standard protocols to assess the quantity and quality of repair tissue and integration with native tissue. Safranin-O with fast green counterstain was used to assess the presence of sulphated glycosaminoglycan (sGAG) within the repair tissue. The area of positively stained sGAG within a region of interest (ROI) in the articular cartilage and subchondral bone regions of the tissue was quantified using Photoshop CS6 [45] (Supplementary Fig. S2). The thickness of cartilaginous repair tissue (measurement of sGAG staining from the joint surface to the interface with subchondral tissue) was quantified ($n = 5$ measurements per defect per animal) (Nikon 239 Microscope Eclipse 90i with NIS Elements Software v3.06, Nikon Instruments Europe, The 240 Netherlands). Haematoxylin and eosin (H&E) staining was used to assess cell arrangement and morphology and tissue formation and integration and new bone formation. The area of bone tissue within an ROI in the subchondral bone region was quantified using Image J (Version 2.0) [46] using an automated method of pixel saturation quantification. Collagen type II was assessed using immunohistochemistry. Briefly, sections were treated with peroxidase, followed by chondroitinase ABC (Sigma–Aldrich) at 37 °C. Sections were incubated with goat serum to block non-specific sites and a collagen type II mouse monoclonal primary antibody (sc-52,658, 1:400, 100 μg/mL, Santa Cruz Biotechnology Inc, TX, USA) was applied for 1 h at 37 °C. Next, the secondary antibody (anti-mouse IgG biotin conjugate, 1:200, 2.1 mg/mL) (Sigma–Aldrich) was added for 1 h, followed by incubation with ABC reagent (Vectastain PK-400, Vector Labs, Peterborough, UK) for 45 min. Finally, sections were developed with DAB peroxidase (Vector Labs) for 5 min. Positive controls (native tissues with primary antibody) and negative controls (native tissues without primary antibody) were included in each batch. Qualitative histological scoring was carried out under blinded conditions using the ICRS II Histological Scoring System (Supplementary Table S2) [47] to provide a comprehensive evaluation of repair tissue within the osteochondral defect sites.

Micro-computed tomography evaluation of bone formation

Micro-computed tomography (micro-CT) analysis was performed on all samples using a Scanco Medical 40 Micro-CT (Bassersdorf, Switzerland) with 70 kVp X-ray source and 112 μA and a voxel resolution of 20 μm to assess the quantity and structure of the new bone formed within the defect site. Samples were maintained in 50% ethanol during scanning. A constrained Gaussian filter was applied to partly suppress noise (filter width (0.8) and filter support (1)). Three-dimensional reconstructions were performed and a threshold of 210 on a scale from 0 to 1000 (399.5 mgHA/cm^3), determined using the method described by Tassini et al. [21], was applied. A volume of interest (VOI) was defined within the subchondral bone as a cylindrical region of 5 × 5 mm and repair was expressed as bone volume per total volume (BV/TV).

Statistical analysis

All statistical analyses were performed using statistics software Prism 6 GraphPad (GraphPad Software, California USA). A Kruskal-Wallis test was applied to assess the statistical significance of ICRS I macroscopic scores. The remaining data was assessed using two-way analysis of variance (ANOVA). Sidak's multiple comparisons test was used to assess statistical differences between the two scaffold groups and Tukey's multiple comparisons test was used to assess statistical differences between the three timepoints. Significance was accepted at a level of $p \leq 0.05$ and results are presented as mean ± standard deviation from the mean.

Results

Clinical observations after scaffold implantation

During surgery, scaffolds were successfully implanted into defects created on the femoral condyle and trochlear ridge (Fig. S3A and B), using the press-fit implantation technique and were seen to fill with blood on implantation (Fig. S3C and D). All animals recovered well postoperatively and within 5 days ambulated freely with no signs of distress or limping for the duration of the study. There were no postoperative complications relating directly to the surgery or the scaffold during the course of the study, and no postoperative infections or patellofemoral dislocations. Assessment of the scaffolds intraoperatively showed that both cell-free and cell-seeded tri-layered scaffolds were easy to handle and no delamination was observed. All scaffolds were successfully implanted, and post surgery recovery was uneventful.

Macroscopic assessment

Macroscopic assessment of the femoral condyle defect site implanted with the cell-free scaffold resulted in median scores of 7.25 out of 12 (range 4 – 9) at 3 months and 6.75 out of 12 (range 4.5 – 9.5) at 6 months, both classified as abnormal (grade III) cartilage (Fig. 1A, B). At 12 months, the macroscopic scores for the cell-free scaffold groups had a median score of 8.5 (range 5.5 – 10) at this site, consistent with nearly normal (grade II) cartilage. The cell-seeded scaffold had a median score of 9 (range 4 – 10) at 3 months (grade II) and scores of 7.25 (range 2

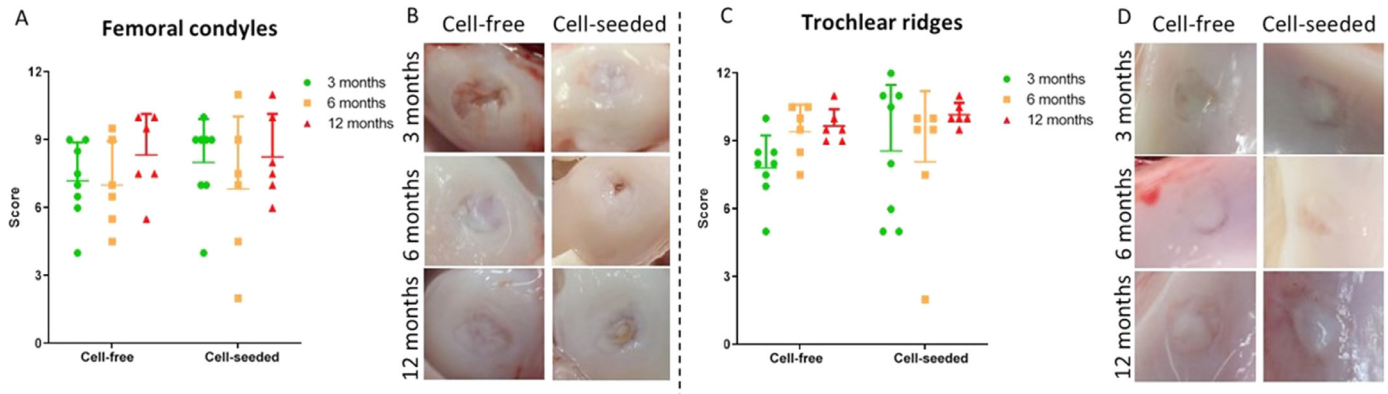

Fig. 1. Macroscopic assessment of femoral condyle and trochlear ridge defect sites following implantation with cell-free or cell-seeded scaffolds. A) Macroscopic scores and B) in situ images of repair tissue in the femoral condyle defects. C) Macroscopic scores and D) in situ images of repair tissue in the trochlear ridge. Results show a trend towards improved cartilage repair over time. Representative images are presented for each group ($n \geq 6$ per group). 8 animals were used per timepoint.

– 11) and 7.75 (range 6 – 11) at 6 (grade III) and 12 months (grade III), respectively (Fig. 1A, B). At the trochlear ridge site, cell-free scaffolds demonstrated median scores of 8 (range 5 – 10), 9.75 (range 7.5 – 10.5) and 9.5 (range 9 – 11) at 3, 6 and 12 months, respectively, all of which were consistent with nearly normal (grade II) cartilage (Fig. 1C, D). Similarly, cell-seeded scaffolds had median scores of 9.25 (range 5 – 12), 9.5 (range 2 – 10) and 10 (range 9.5 – 11) at 3, 6 and 12 months, respectively, also consistent with nearly normal (grade II) cartilage (Fig. 1C, D). While the results showed a general trend towards improved macroscopic scores between the 3 month and 12 month timepoints and a reduction in variability between samples, particularly in the trochlear ridge defect sites, due to the high level of variability no significant difference in the overall macroscopic appearance was found between the repair tissue in the defect sites treated with the cell-free and cell-seeded scaffolds.

Histological assessment

Safranin-O histological staining of femoral condyles indicated a degree of intragroup variation in defects treated with both cell-free and cell-seeded scaffolds at the 3 month and 6 month timepoints (Fig. 2A). At the 12 month timepoint for this defect site, differences between high-ranked and low-ranked samples within scaffold groups were much less pronounced, with high-ranked samples in both groups demonstrating full regeneration of the articular surface accompanied by the establishment of a tidemark. In mid-ranked samples, small fissures in the articular surface were observed, while low-ranked samples demonstrated chondral regions which had low levels of sGAG staining. Histomorphometric quantification of sGAG within the chondral regions of femoral condyle defects showed no significant difference in sGAG between cell-free and cell-seeded groups (Fig. 2B). sGAG staining was significantly higher at the 3 month timepoint than at 6 and 12 months in cell-free groups (49.50 ± 13.53% vs. 20.66 ± 13.73% and 19.96 ± 12.32%; $p \leq 0.01$), whereas no significant difference in sGAG staining was observed within the chondral region in the cell-seeded group between the three timepoints. Immunohistochemistry performed on femoral condyle defects demonstrated weak staining for collagen type II in the cell-free group at 3 months, with stronger staining observed at this timepoint in the cell-seeded group (Fig. 2C). At 12 months, the cartilage morphology of both cell-free and cell-seeded scaffold groups was observed to be more hyaline-like compared to earlier timepoints at this defect site and similar to the native tissue control. Overall, the histological analysis showed higher levels of staining in the cell-seeded group at 12 months compared to the cell-free group, indicating higher quality cartilage repair in this group. However, while sGAG quantification showed an overall trend towards higher levels of sGAG in the cell-seeded group at 6 and 12 months, this was not significant.

In the trochlear ridge site, intense staining for safranin-O was observed throughout defects treated with both cell-free and cell-seeded scaffolds at 3 months (Fig. 2D). At 6 months in both groups, high and mid-ranked samples demonstrated good levels of regeneration at the articular surface, while in low-ranked samples reduced sGAG staining was observed in the chondral layer and fibrous tissue was observed in the subchondral layer. At 12 months, higher levels of sGAG staining were observed in the cell-seeded group compared to the cell-free group, with lower levels of intragroup variation observed compared to earlier timepoints. Similar to the femoral condyle site, a significant reduction in sGAG staining was observed in the cell-free group between the 3 month and the 6 and 12 month timepoints (35.96 ± 8.12% vs 17.87 ± 10.36%, $p \leq 0.05$ and 8.75 ± 10.8%; $p \leq 0.001$), whereas in the cell-seeded group this reduction in sGAG was again not observed (Fig. 2E). Again, while higher levels of sGAG staining were observed in the cell-seeded group at 12 months, the finding was not significant. At the trochlear ridge defect site, the intensity of collagen type II immunohistochemical staining increased over time in both groups and by 12 months a well-integrated layer of articular cartilage, similar to native controls, could be observed in both cell-free and cell-seeded groups (Fig. 2F).

Next, the levels of bone regeneration within the subchondral region of defects were examined. At the femoral condyle site, histomorphometric quantification of bone formation from H&E stained slides showed no significant differences in bone regeneration between the cell-free and cell-seeded scaffold groups (Fig. 3A and C). However, it was noted that there was a trend towards higher levels of new bone formation in the cell-free group compared to the cell-seeded group at the 6 month time point ($p = 0.0703$). Within the cell-free group there was a significant increase in bone repair tissue at 6 months (31.71 ± 11.41% vs. 16.65 ± 10.03%; $p = 0.0398$) and 12 months (31.48 ± 14.12% vs. 16.65 ± 10.03%; $p = 0.0436$) compared to 3 months. In the cell-seeded group, however, no significant increase in bone formation was observed between 3 and 6 months, with significant increases occurring instead at 12 months compared to the 6 month (41.59 ± 9.85% vs. 17.77 ± 14.11%: $p \leq 0.01$) and 3 month timepoints (41.59 ± 9.85% vs. 10.68 ± 7.87%; $p \leq 0.0001$). This points towards a delay in bone regeneration in the cell-seeded group at this defect site. Quantification of sGAG staining within the subchondral bone region showed a reduction in sGAG staining over time corresponding to the rate of new bone formation (Fig. 3E). Interestingly, however, this reduction was only significant in the cell-free group (3 months vs. 12 months; 24.89 ± 21.3% vs. 3.34 ± 3.69; $p = 0.0268$), indicating that cartilage matrix in the subchondral bone region persisted to a greater degree in the cell-seeded group.

At the trochlear ridge site, H&E staining indicated a similar progression in bone regeneration in both the cell-free and cell-seeded group with no significant differences observed between scaffold groups at any

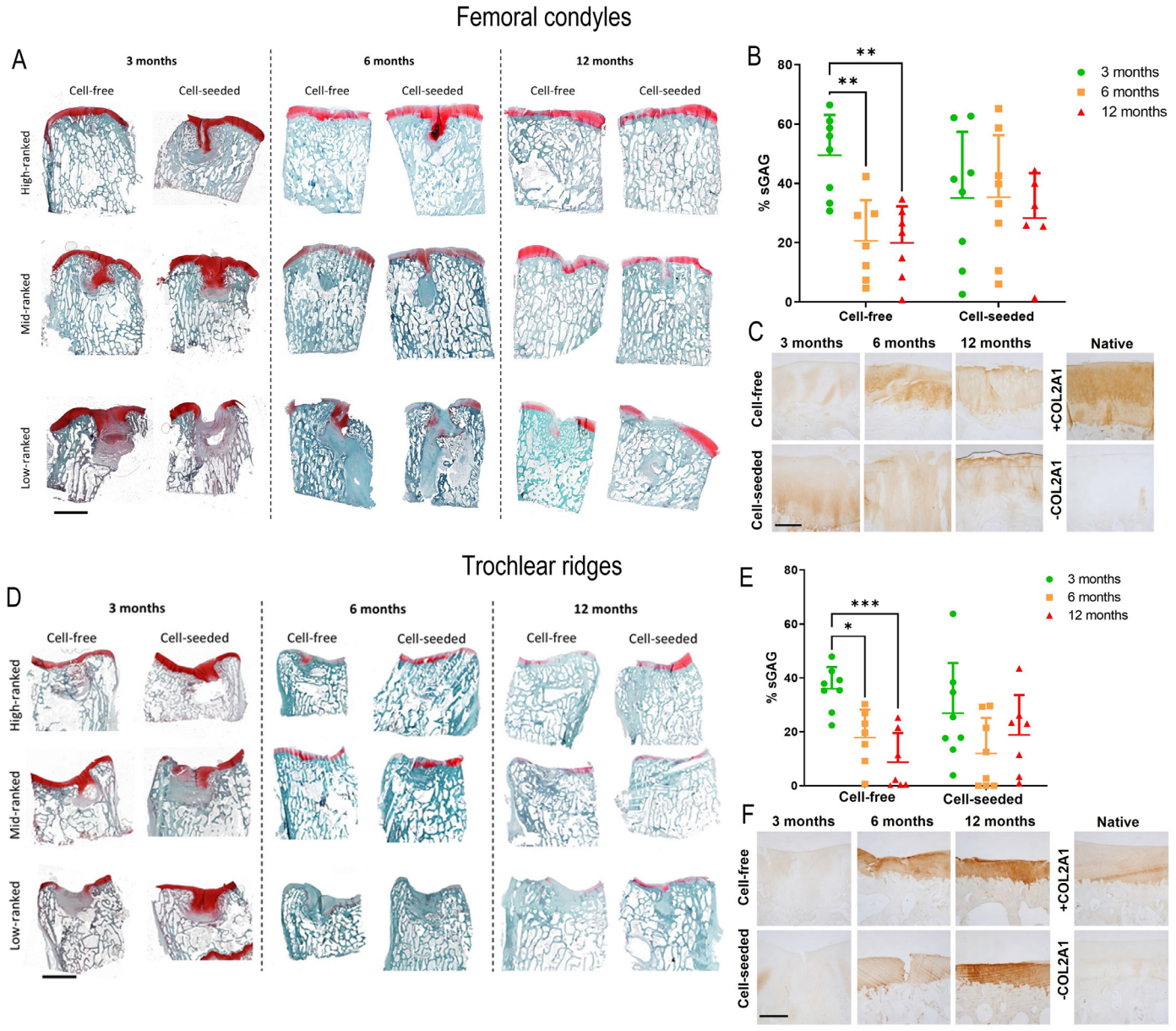

Fig. 2. Histological assessment of cartilage repair in the femoral condyle defect (A,B,C) and trochlear ridge defect sites (D,E,F). A) Safranin-O histological staining of femoral condyle defects treated with either cell-free or cell-seeded scaffolds. High, mid, and low-ranked samples, determined according to the ICRS II histological scoring system, are presented for each timepoint. Scale bar – 5 mm. B)% GAG calculated in the chondral region of femoral condyle defects (** $p \leq 0.01$) ($n \geq 6$ per group). C) Collagen type II immunohistochemistry of femoral condyle defects treated with either cell-free or cell-seeded scaffolds. Native controls both with (+) and without (-) the primary antibody (COL2A1) added were included in each batch. Scale bar – 500 μm. D) Safranin-O histological staining of trochlear ridge defects treated with either cell-free or cell-seeded scaffolds. High, mid, and low-ranked samples, determined according to the ICRS II histological scoring system, are presented for each timepoint. Scale bar – 5 mm. E)% GAG calculated in the chondral region of the trochlear ridge defects (* $p \leq 0.05$, *** $p \leq 0.001$) ($n \geq 6$ per group). F) Collagen type II immunohistochemistry of trochlear ridge defects treated with either cell-free or cell-seeded scaffolds. High-ranked samples are presented for each group. Native controls both with (+) and without (-) the primary antibody (COL2A1) added were included in each batch. Scale bar – 500 μm. 8 animals were used per timepoint.

time point (Fig. 3B and D). Cell-free scaffolds demonstrated significantly higher levels of new bone formation at 6 months (27.20 ± 11.08% vs. 11.646 ± 7.10%; $p \leq 0.01$) and 12 months (37.6 ± 9.07% vs. 11.646 ± 7.10%; $p \leq 0.0001$) compared to the 3 month timepoint (Fig. 3D). Similarly, in the cell-seeded group, bone repair tissue increased significantly over the time frame of the study. At 6 months significantly higher levels of bone were present in the defect site compared to 3 months (20.79 ± 11.89% vs. 8.92 ± 6.85%; $p \leq 0.05$) and at 12 months compared to 6 months (33.76 ± 8.45% vs. 20.79 ± 11.89%; $p \leq 0.05$) and 3 months (33.76 ± 8.45% vs. 8.92 ± 6.85%; $p \leq 0.0001$). Quantification of sGAG staining within the subchondral bone region showed a corresponding reduction in sGAG staining over time as new bone formed with significantly lower levels of sGAG staining at the 6 month and 12 month timepoints compared to the 3 month timepoint in both the cell-free and cell-seeded groups (Fig. 3F).

μCT evaluation of bone regeneration

Bone regeneration within the defect sites was then assessed using μCT, whereby explanted defects were scanned and a cylindrical region of 5 × 5 mm was defined within the defect site in order to calculate bone volume per total volume (BV/TV). μCT reconstructions at both femoral

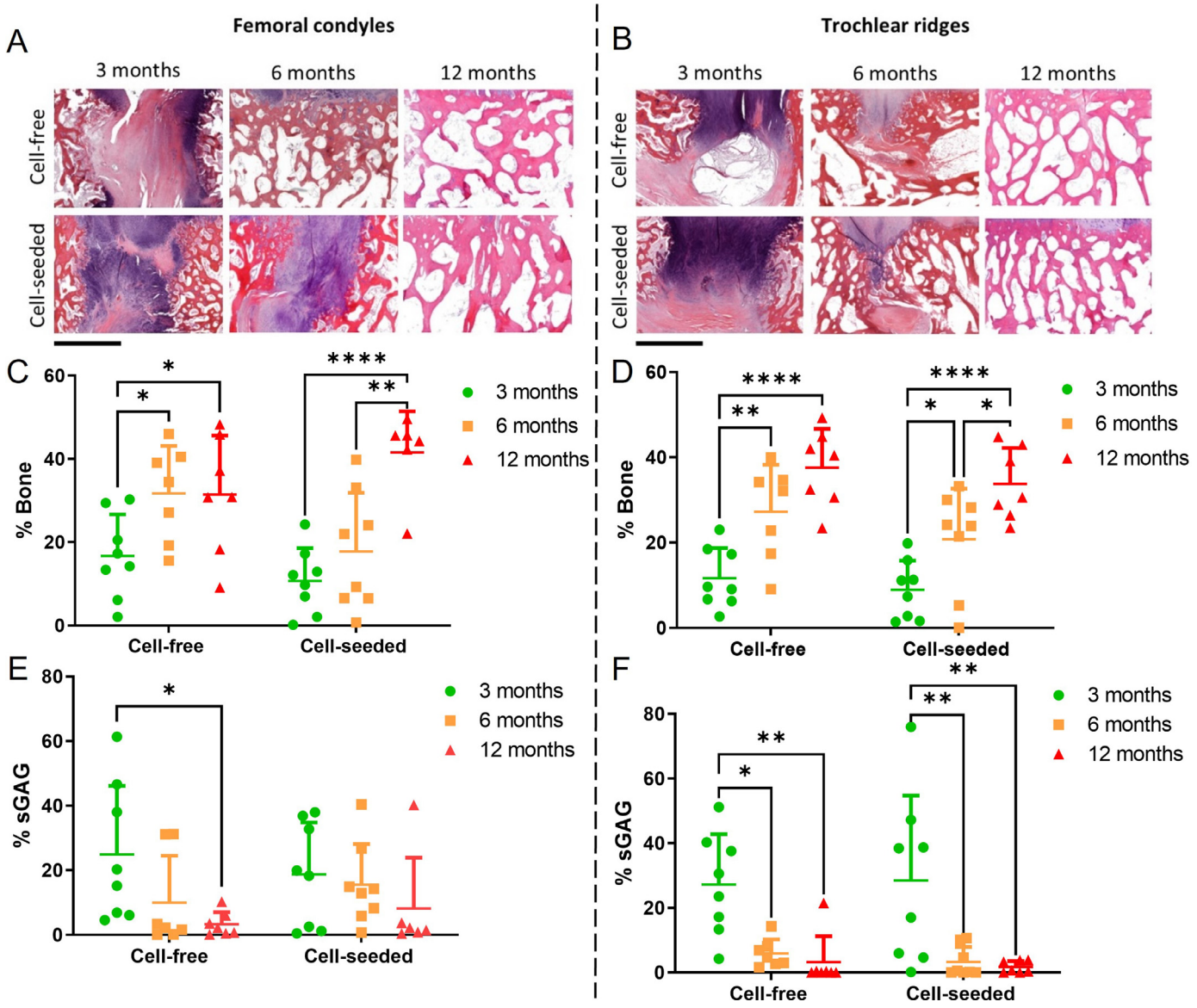

Fig. 3. Histological assessment of bone repair in the femoral condyle and trochlear ridge defect sites. H&E staining of the subchondral region treated with either cell-free or cell-seeded scaffolds in A) femoral condyle defects and B) trochlear ridge defects. Representative images are presented for each group. Scale bar – 2 mm.% Bone repair tissue calculated within the subchondral region of C) femoral condyle defects and D) trochlear ridge defects ($n \geq 6$ per group). Quantification of GAG staining in subchondral bone region of E) femoral condyle defects and F) trochlear ridge defects. Significance; $^{*}p \leq 0.05$, $^{**}p \leq 0.01$, $^{***}p \leq 0.001$, $^{****}p \leq 0.0001$. 8 animals were used per timepoint.

condyle and trochlear ridge sites demonstrated near full regeneration of defects treated with both the cell-free and cell-seeded scaffolds at 12 months (Fig. 4A, B), demonstrating the ability of both scaffold groups to effectively promote bone repair. No significant difference in the rate of bone formation was observed at earlier timepoints. In both the cell-free and cell-seeded groups in both defect sites the BV/TV was significantly higher at 12 months compared to 3 months (Fig. 4C, D). In the femoral condyle site, the BV/TV at 3 months was 0.24 ± 0.12 compared to 0.43 ± 0.09 at 12 months ($p \leq 0.01$) in the cell-free group and 0.167 ± 0.11 at 3 months compared to 0.41 ± 0.083 at 12 months ($p \leq 0.001$) in the cell-seeded group (Fig. 4C). At the trochlear ridge site, the BV/TV was 0.23 ± 0.09 at 3 months and 0.45 ± 0.14 at 12 months ($p \leq 0.01$) in the cell-free group and 0.15 ± 0.05 at 3 months and 0.44 ± 0.08 at 12 months in the cell-seeded group ($p \leq 0.001$) (Fig. 4D). Although not statistically significant, BV/TV values were lower at 3 and 6 months in the cell-seeded compared to the cell-free group in both defect sites, potentially indicating that new bone formation occurred more slowly in the defects treated with the cell-seeded scaffold.

ICRS II evaluation of regenerated cartilage and bone

Cartilage and bone tissue regeneration within the femoral condyle and trochlear ridge defect sites were further assessed using the ICRS II histological scoring tool (Fig. 5A, C). Representative cross-sectional images of repair tissue within the femoral condyle (Fig. 5B) and trochlear ridge defect sites (Fig. 5D) are also shown. While no significant differences in ICRS II scores are observed in the femoral condyle defect, in the trochlear ridge defect treated with the cell-seeded scaffold significantly higher ICRS II scores are reported at 12 months compared to the 3 month timepoint (1110.0 ± 175.69 vs. 855.56 ± 68.39 ($p \leq 0.05$). Examination of the individual ICRS II categories again showed no significant differences between the cell-free and cell-seeded groups in either defect site. However, the results showed that scores for tidemark for-

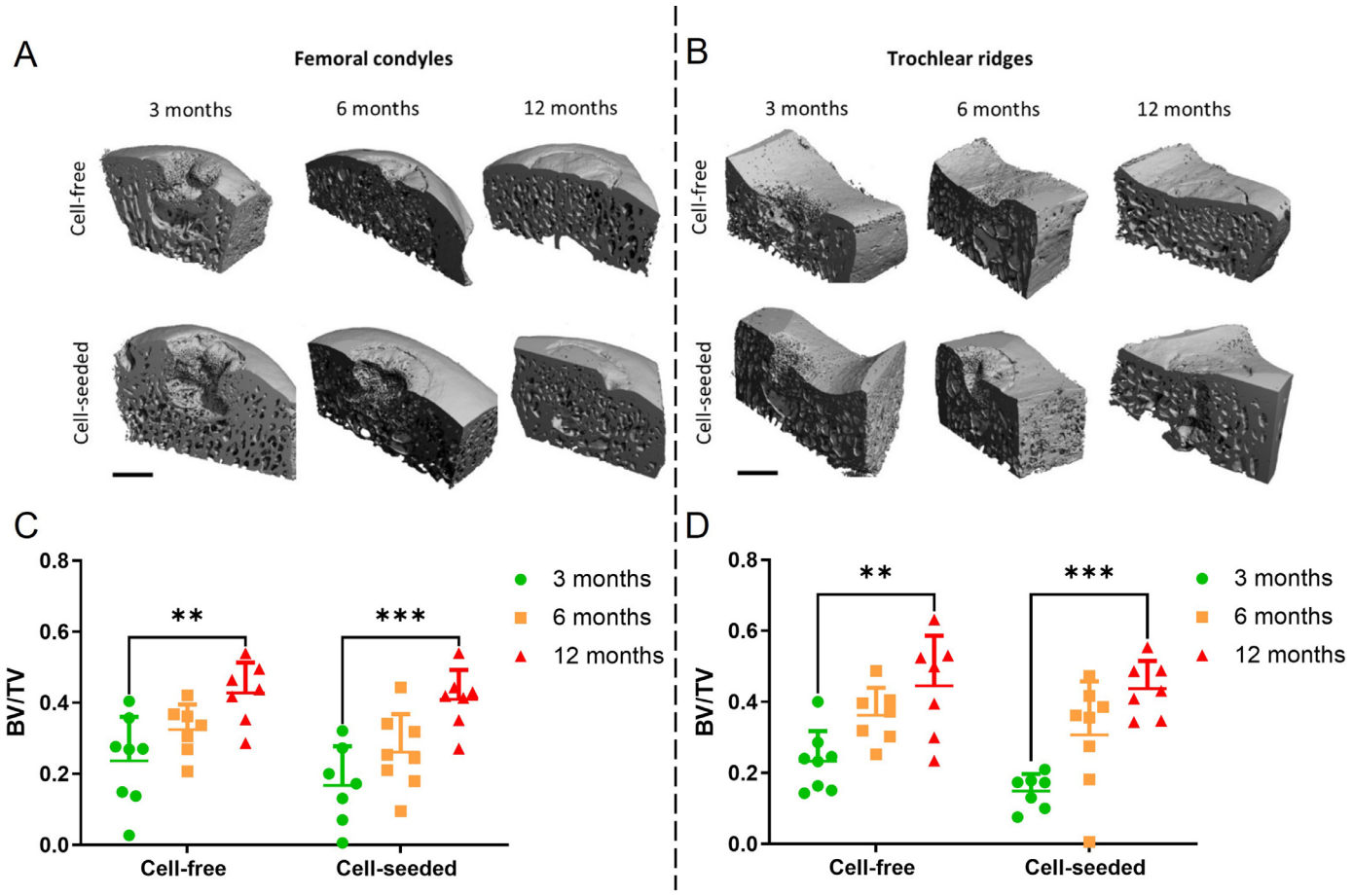

Fig. 4. μCT evaluation of bone regeneration. Representative μCT reconstructions depicting cross-sections of A) femoral condyle defects and B) trochlear ridge defects treated with either cell-free or cell-seeded scaffolds at 3, 6 and 12 month timepoints. Scale bar – 3 mm. BV/TV of C) femoral condyle defects and D) trochlear ridge defects treated with cell-free or cell-seeded scaffolds at 3, 6 and 12 month timepoints ($n \geq 6$ per group). Significance; $^{**}p \leq 0.01$, $^{***}p \leq 0.001$. 8 animals were used per timepoint.

mation (Fig. S5C and Fig. 9C) S6nd mid-deep zone assessment (Fig. S5F and Fig. S6F) in the cell-seeded group in both defect sites were lower at 3 months than in the corresponding cell-free group, but increased significantly over time. Furthermore, the score for matrix staining of cell-free scaffolds in the trochlear ridge site was significantly lower at 12 months compared to 3 months ($p \leq 0.05$) (Fig. 9A). Scores for subchondral bone abnormalities were lower in the cell-seeded group than in the cell-free group in both defects sites at 3 and 6 months but, unlike the cell-free group, the cell-seeded group scored significantly higher at 12 months compared to 3 months indicating an improvement in subchondral bone quality over time ($p \leq 0.05$) (Fig. S5D and Fig. S6D).

Discussion

Tissue engineering approaches have been widely explored for the treatment of cartilage and osteochondral defects, with biomaterial-based scaffolds emerging as an effective off-the-shelf treatment. Seeding scaffolds with cells offers the potential to further enhance tissue regeneration, although this brings limitations relating to cost and ease of surgical application [48]. This work sought to explore whether the regenerative potential of a biomimetic tri-layered scaffold with proven regenerative potential could be enhanced by incorporating a chondrogenic cell population. To explore this hypothesis, cell-free and cell-seeded tri-layered scaffolds were implanted in osteochondral defects created on the femoral condyle and the trochlear ridge in a translational, large animal model. Specifically, co-cultures of CCs and FPMSCs harvested utilizing rapid cell isolation techniques were employed. The results from macroscopic assessment, histological assessment and μCT analysis demonstrated that both the cell-free and cell-seeded treatment approaches achieved effective repair of osteochondral defects with the formation of a defined tidemark by the 12 month timepoint. The analysis showed trends towards improved cartilage repair in the cell-seeded scaffold group, however, no significant differences were observed between the cell-free and cell-seeded groups and a delay in subchondral bone healing was observed in the cell-seeded scaffold group compared to the cell-free group. Taking into consideration the additional cost and complexity associated with the cell-seeded scaffold approach, this study demonstrates that the treatment of osteochondral defects using cell-free scaffolds represents the preferred clinical approach.

For eventual clinical translation, demonstration of the ability of biomaterial scaffolds to generate good quality cartilage and integrate with the underlying bone in a large animal in vivo model is crucial. Although the scaffold might stimulate mineralisation and cartilage formation in vitro there are many other factors in an in vivo situation, such as biomechanical effects due to weight-bearing, as well as circulating stimulating and inflammatory factors, that may help or hinder the result. Therefore, in order to evaluate the efficacy of a cell-seeded tri-layered scaffold, we selected a well established clinically relevant goat model which was previously leveraged by our group to demonstrate the capacity of a cell-free tri-layered scaffold to promote cartilage regeneration over defects left empty and a leading commercial comparator [21]. In many cases, cartilage repair procedures result in mechanically inferior fibrocartilage which tends to degenerate over time [49]. Thus, in order to assess the extent of regeneration of the articular cartilage and quality of the repair

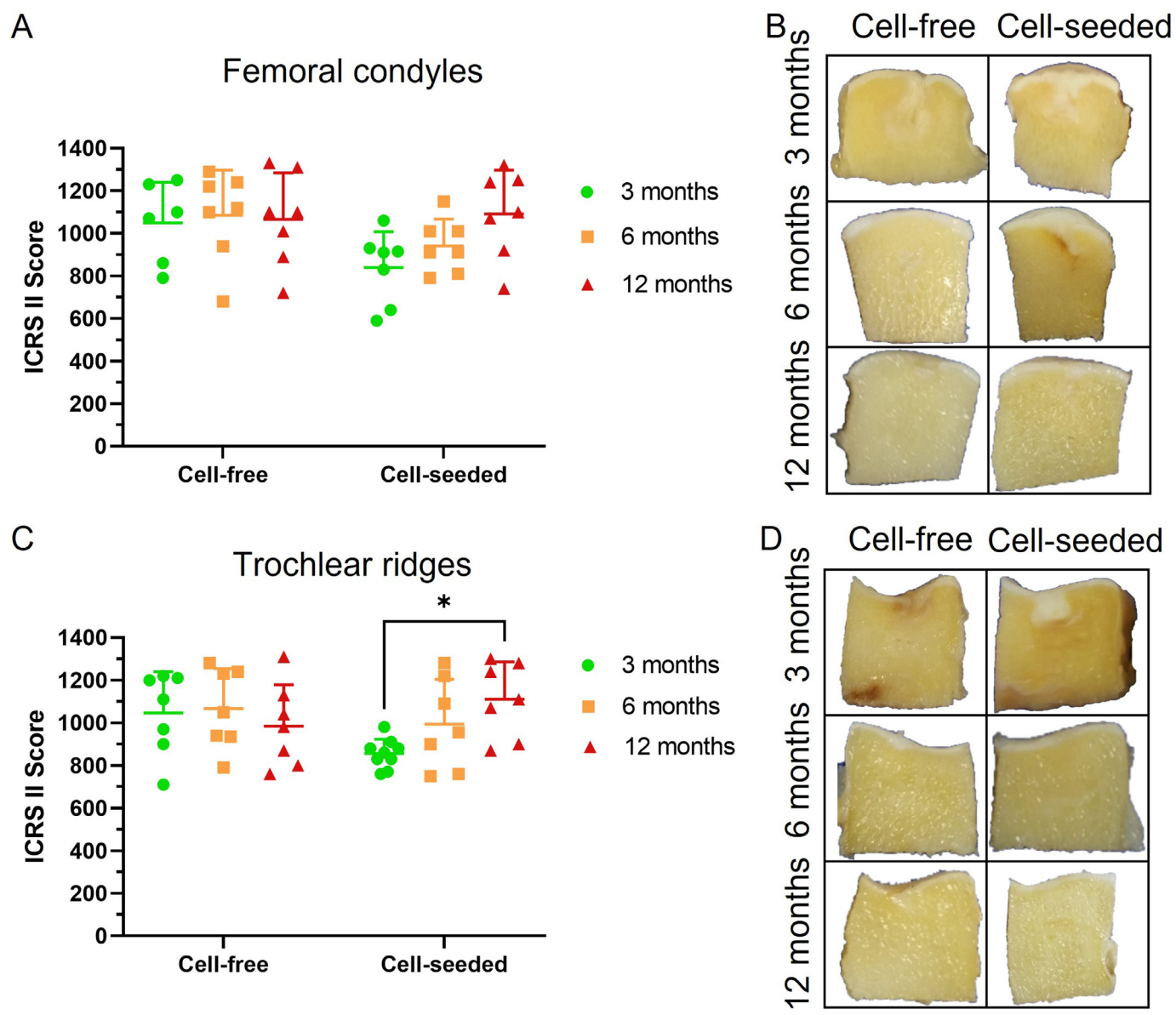

Fig. 5. Overall ICRS II scores for femoral condyle and trochlear ridge defect sites at 3, 6 and 12 months. A) ICRS II scores for femoral condyle defects treated with either cell-free or cell-seeded scaffolds. B) Cross-sectional images of femoral condyle defects. C) ICRS II scores for trochlear ridge defects treated with either cell-free or cell-seeded scaffolds. D) Cross-sectional images of trochlear ridge defects. Representative images are presented for each group ($n \geq 6$ per group). Significance; * $p \leq 0.05$. 8 animals were used per timepoint.

tissue, repair was assessed at an early timepoint of 3 months and later timepoints of 6 and 12 months post-implantation.

Initial assessment of repair tissue within the defect sites was carried out using the ICRS macroscopic evaluation tool. Within the femoral condyle defect site, the cell-free scaffold group showed the formation of nearly normal cartilage (ICRS grade II) by the 12 month timepoint. For the cell-seeded scaffold group a grade II, nearly normal cartilage, score was observed at 3 and 6 months in this defect site, suggesting that the chondrocyte/FPMSC co-culture may be beneficial in promoting early tissue repair. However, these differences were not statistically significant and were not maintained to the 12 month timepoint. At all three timepoints (3, 6 and 12 months) in the trochlear ridge site, both the cell-free and cell-seeded groups demonstrated the ability to regenerate a joint surface that appeared "nearly normal", scoring between 8 and 11 out of 12 based on the ICRS score, and showed evidence of good defect repair and cartilage integration with a macroscopically smooth articular surface.

Histomorphometry was then used to investigate changes in matrix synthesis within, and between, scaffold groups over time. To that end, we defined a chondral region encompassing the articular cartilage layer of the defect as a rectangular area1.5 mm in height x 5 mm in width, and determined the degree of sGAG present within the matrix through the quantification of safranin-O histological staining. The results showed that both cell-free and cell-seeded scaffolds demonstrated high levels of sGAG in the chondral layer at 3 months, with higher sGAG levels maintained in the cell-seeded group compared to the cell-free group over the 6 and 12 month timepoints. Similar results were observed irrespective of the anatomical site used. High concentrations of glycosaminoglycans, particularly hyaluronic acid, are reportedly found at the early stages of cartilage repair to aid cellular migration into the repair site and subsequent proliferation [50] and thus aid in the generation of stable cartilage tissue. These results therefore potentially indicate an increase in sGAG production in the cell-seeded scaffold groups as a result of the addition of the chondrogenic cell population. In both cases, the decreases

in sGAG content were mirrored by increases in collagen type II matrix synthesis. Positive collagen type II staining, similar to that of native tissue, was observed in both scaffold groups at the 12 month timepoint in both defect sites, with stronger staining observed in the trochlear ridge defects. Collagen type II is a key marker of stable hyaline articular cartilage and thus this result indicates the capability of both the cell-free and cell-seeded scaffolds to promote the regeneration of damaged hyaline cartilage tissue.

Regeneration of the underlying subchondral bone is another key component of osteochondral defect repair. In order to assess levels of bone repair, histomorphometry was performed to quantify new bone formation and the presence of sGAG within the subchondral region, defined as a rectangular area of height 3.5 mm and width 5 mm located immediately below the chondral region described above. The results showed an increase in new bone formation in both scaffold groups in both defect sites. However, new bone formation appears delayed in the cell-seeded groups at early timepoints. High levels of sGAG staining were observed in the early stages of the bone repair process indicating that bone repair occurred through the process of endochondral ossification i.e., the replacement of an initial cartilaginous template with bone [51–53]. By the 12 month timepoint, complete repair of the subchondral bone with the formation of a tidemark was observed in all groups. These results were supported by BV/TV quantification using μCT. Histologically the newly formed bone at 12 months appeared to be of high quality without the presence of bone voids or bone cysts that are frequently reported in other studies [54,55]. While not statistically significant, it was noted from both histomorphometry and μCT that higher levels of new bone formation had occurred by the 3 and 6 months timepoints in the cell-free scaffold groups compared to the cell-seeded groups in both defect sites. Interestingly, for cell-free scaffolds implanted in the femoral condyle site, a delay in subchondral bone regeneration was accompanied by greater persistence of cartilage matrix, which potentially indicates that the use of a chondrogenic cell population in the adjacent chondral region plays a role in regulating the conversion of cartilage to bone in the subchondral region.

Evaluation of repair tissue using the ICRS II histological scoring system again showed similar levels of repair between the cells-free and cell-seeded scaffolds in both defect sites. On examining the scores in individual categories within the ICRS II scoring system it was observed that in both defect sites there was a trend towards lower scores in bone repair related categories, such as formation of tidemark, subchondral bone abnormalities and mid-deep zone assessment, in the cell-seeded group at the 3-month timepoint compared to the cell-free scaffold group, again indicating that the inclusion of a chondrogenic cell population within the scaffolds delayed the normal bone healing processes. Furthermore, the significant reduction in matrix staining observed in cell-free scaffolds in the trochlear ridge was not observed in cell-seeded scaffolds. These findings appear to support the results demonstrated by cartilage and bone histomorphometry, with cartilage matrix in the chondral area decreasing over time in the cell-free group whilst remaining stable in the cell-seeded group, and subchondral bone regeneration occurring more slowly initially in the cell-seeded group but increasing over the 12 month observation period to match or surpass levels reached in the cell-free group.

It was noted that while subchondral bone repair in the cell-free group was similar between the femoral condyle and trochlear ridge defect sites, the rate of repair and quality of repair of cartilage tissue was better in the trochlear ridge defect site. This reflects differences in repair between the femoral condyle and the trochlear ridge that have been seen previously and are likely due to the higher weight-bearing in the femoral condyle during normal ambulation [25]. This finding is important because although the vast majority of clinically important osteochondral defects are found on the femoral condyle or other weight-bearing portions of the joint, a period of reduced loading is generally followed post-operatively which is not practical to replicate in goats [5,56,57].

One potential limitation of this study was the use of allogeneic cells, necessary due to limitations in equipment and on-site facilities. Allogenic FPMSCs have been successfully used for cartilage repair applications previously without eliciting a negative immune response [58,59]. However, these studies were carried out in rabbit models using genetically similar laboratory rabbits. While no evidence of any negative effects resulting from the use of allogenic cells was noted at the timepoints investigated, it is possible that an early inflammatory response interrupted the healing process and may have been responsible for the generally poorer subchondral bone regeneration at earlier timepoints. The approach described in this paper envisages the use of autologous cells which would be harvested from the patient and subsequently seeded onto the scaffold for implantation without the requirement for an in vitro expansion phase. It is therefore evident that the next step in this work should be to investigate whether regenerative outcomes could be further improved through the use of autologous cells, while also considering that an increase in cell-seeding density may also be required to drive regeneration in an in vivo environment. Additionally, longer-term studies are required to demonstrate whether the cartilage generated by cell-seeded scaffolds in this study persists over time, to achieve more robust repair of osteochondral defects. Furthermore, the use of cell-tracing would aid in elucidating the fate of implanted cells and their role in the tissue repair process.

In this work, we sought to provide a framework for future cell-based tissue engineering approaches which aim to circumvent the in vitro cell expansion phase associated with current cell-based therapies, such as ACI. The study shows that both the cell-free and cell-seeded treatment approaches achieved effective repair of osteochondral defects, nonetheless, a clear benefit from the use of the cell-based approach described herein was not observed. This may be due to the success of this scaffold in promoting the infiltration of native cells, potentially masking the benefit of the seeded cell population. Taking this into consideration with the additional cost and complexity associated with the cell-seeded scaffold approach, this study demonstrates that the treatment of osteochondral defects using cell-free scaffolds remains the preferred clinical approach.

Conclusions

This study demonstrates that biomimetic tri-layered scaffolds implanted, both cell-free and seeded with a rapidly isolated CC/FPMSC co-culture, into osteochondral defects in a caprine model promoted the repair of bone and cartilage tissue within the defect site. The results indicated a delay in subchondral bone healing in the cell-seeded groups, however, by the 12 month time point the cell-free and allogenic cell-seeded scaffolds yield regenerated cartilage and bone tissues with comparable quality and quantity. Overall, the results of the study reinforce the potential of the biomimetic tri-layered scaffold to repair joint defects but failed to demonstrate a clear benefit from the addition of the CC/FPMSC co-culture to this scaffold, indicating that the treatment of osteochondral defects using cell-free scaffolds represents a more prudent clinical approach.

Supplementary data

Figure S1. Fabrication process for the tri-layered scaffold

Figure S2. Safranin-O staining of native femoral condyle illustrating the regions used for histomorphometry. The chondral region was defined as a rectangular area of height 1.5 mm and width 5 mm. The subchondral region was defined as a rectangular area of height 3.5 mm and width 5 mm.

Figure S3: Creation of femoral condyle and trochlear ridge defects. 6 mm x 6 mm defects created on A) medial femoral condyle and B) trochlear ridge. Tri-layered scaffolds implanted using the press-fit implantation technique into both C) the medial femoral condyle and D) the trochlear ridge filled with blood on implantation.

Figure S4: ICRS I macroscopic scores for individual categories for femoral condyle (A) and trochlear ridge (B) defects ($n \geq 6$). Results are presented as the median score with individual data points. 8 animals were used per timepoint.

Figure S5. ICRS II histological scores for the femoral condyle. A) Matrix staining, B) Surface Architecture, C) Formation of Tidemark, D) Subchondral Bone Abnormalities, E) Surface/Superficial Assessment and F) Mid-Deep Zone ($n \geq 6$). * $p \leq 0.05$. Results are presented as the median score with individual data points. 8 animals were used per timepoint.

Figure S6: ICRS II histological scores for the trochlear ridge. A) Matrix staining, B) Surface Architecture, C) Formation of Tidemark, D) Subchondral Bone Abnormalities, E) Surface/Superficial Assessment and F) Mid-Deep Zone ($n \geq 6$). Significance; * $p \leq 0.05$, ** $p \leq 0.01$. 8 animals were used per timepoint.

Table S1: International Cartilage Repair Society (ICRS) cartilage repair assessment tool. This tool is used by surgeons to evaluate the macroscopic appearance of cartilage repair tissue following interventions such as ACI, subchondral drilling and microfracture.

Table S2: Histological scoring of repair tissue in defects treated with cell-free and cell-seeded scaffold groups was carried out using the International Cartilage Repair Society (ICRS) II scoring system. The scoring system comprises 14 parameters with each criterion evaluated based on the visual analogue scale and graded from 0 to 100.

Declaration of Competing Interest

Authors TJ Levingstone and FJ O'Brien hold IP with a commercial product of related composition to the collagen-based scaffolds used in this study.

Data Availability

Data will be made available on request.

Funding

This work was supported by Science Foundation Ireland (SFI)/ Health Research Board (HRB) Translational Research Award (TRA/2011/19), the EU BlueHuman Interreg Atlantic Area Project (EAPA_151/2016), the European Research Council (grant agreement no. 788,753-ReCaP) and the Irish Research Council (GOIPG/2015/3186) for funding.

Supplementary materials

Supplementary material associated with this article can be found, in the online version, at doi:10.1016/j.bbiosy.2022.100066.

References

[1] Woolf AD, Pfleger B. Burden of major musculoskeletal conditions. Bull World Health Organ 2003;81(9):646–56.
[2] Steadman JR, Rodkey WG, Rodrigo JJ. Microfracture: surgical technique and rehabilitation to treat chondral defects. Clin Orthop Relat Res 2001(391 SUPPL):S362–9.
[3] Mithoefer K, McAdams T, Williams RJ, Kreuz PC, Mandelbaum BR. Clinical efficacy of the microfracture technique for articular cartilage repair in the knee: an evidence-based systematic analysis. Am J Sports Med 2009;37(10):2053–63.
[4] Breinan HA, Martin SD, Hsu H-P, Spector M. Healing of canine articular cartilage defects treated with microfracture, a type-II collagen matrix, or cultured autologous chondrocytes. J Orthop Res 2000;18(5):781–9.
[5] Hangody L, Vasarhelyi G, Hangody LR, Sukosd Z, Tibay G, Bartha L, Bodo G. Autologous osteochondral grafting–technique and long-term results. Injury 2008;39(Suppl 1):S32–9.
[6] Hangody L, Kish G, Karpati Z, Udvarhelyi I, Szigeti I, Bely M. Mosaicplasty for the treatment of articular cartilage defects: application in clinical practice. Orthopedics 1998;21(7):751–6.
[7] Bexkens R, Ogink PT, Doornberg JN, Kerkhoffs GMMJ, Eygendaal D, Oh LS, van den Bekerom MPJ. Donor-site morbidity after osteochondral autologous transplantation for osteochondritis dissecans of the capitellum: a systematic review and meta-analysis. Knee Surg Sports Traumatol Arthrosc 2017;25(7):2237–46.
[8] Brittberg M, Lindahl A, Nilsson A, Ohlsson C, Isaksson O, Peterson L. Treatment of deep cartilage defects in the knee with autologous chondrocyte transplantation. New Engl J Med 1994;331(14):889–95.
[9] Li MH, Xiao R, Li JB, Zhu Q. Regenerative approaches for cartilage repair in the treatment of osteoarthritis. Osteoarthritis Cartilage 2017;25(10):1577–87.
[10] Bhosale AM, Richardson JB. Articular cartilage: structure, injuries and review of management. Br Med Bull 2008;87(1):77–95.
[11] Minas T, Ogura T, Bryant T. Autologous chondrocyte implantation. JBJS Essent Surg Tech 2016;6(2) e24-e24.
[12] Samuelson EM, Brown DE. Cost-effectiveness analysis of autologous chondrocyte implantation: a comparison of periosteal patch versus type I/III collagen membrane. Am J Sports Med 2012;40(6):1252–8.
[13] Diaz-Romero J, Gaillard JP, Grogan SP, Nesic D, Trub T, Mainil-Varlet P. Immunophenotypic analysis of human articular chondrocytes: changes in surface markers associated with cell expansion in monolayer culture. J Cell Physiol 2005;202(3):731–42.
[14] Barbero A, Grogan S, Schäfer D, Heberer M, Mainil-Varlet P, Martin I. Age related changes in human articular chondrocyte yield, proliferation and post-expansion chondrogenic capacity. Osteoarthritis Cartilage 2004;12(6):476–84.
[15] Schnabel M, Marlovits S, Eckhoff G, Fichtel I, Gotzen L, Vécsei V, Schlegel J. Dedifferentiation-associated changes in morphology and gene expression in primary human articular chondrocytes in cell culture. Osteoarthritis Cartilage 2002;10(1):62–70.
[16] Lim HC, Bae JH, Song SH, Park YE, Kim SJ. Current treatments of isolated articular cartilage lesions of the knee achieve similar outcomes. Clin Orthop Relat Res 2012;470(8):2261–7.
[17] Gou GH, Tseng FJ, Wang SH, Chen PJ, Shyu JF, Weng CF, Pan RY. Autologous chondrocyte implantation versus microfracture in the knee: a meta-analysis and systematic review. Arthroscopy 2020;36(1):289–303.
[18] Levingstone TJ, Matsiko A, Dickson GR, O'Brien FJ, Gleeson JP. A biomimetic multi-layered collagen-based scaffold for osteochondral repair. Acta Biomater 2014;10(5):1996–2004.
[19] Stack JD, Levingstone TJ, Lalor W, Sanders R, Kearney C, O'Brien FJ, David F. Repair of large osteochondritis dissecans lesions using a novel multilayered tissue engineered construct in an equine athlete. J Tissue Eng Regen Med 2017;11(10):2785–95.
[20] Levingstone TJ, Thompson E, Matsiko A, Schepens A, Gleeson JP, O'Brien FJ. Multi-layered collagen-based scaffolds for osteochondral defect repair in rabbits. Acta Biomater 2016;32:149–60.
[21] Levingstone TJ, Ramesh A, Brady RT, Brama PAJ, Kearney C, Gleeson JP, O'Brien FJ. Cell-free multi-layered collagen-based scaffolds demonstrate layer specific regeneration of functional osteochondral tissue in caprine joints. Biomaterials 2016;87:69–81.
[22] Kafienah W, Jakob M, Demarteau O, Frazer A, Barker MD, Martin I, Hollander AP. Three-dimensional tissue engineering of hyaline cartilage: comparison of adult nasal and articular chondrocytes. Tissue Eng 2002;8(5):817–26.
[23] Vinatier C, Gauthier O, Fatimi A, Merceron C, Masson M, Moreau A, Moreau F, Fellah B, Weiss P, Guicheux J. An injectable cellulose-based hydrogel for the transfer of autologous nasal chondrocytes in articular cartilage defects. Biotechnol Bioeng 2009;102(4):1259–67.
[24] Leijten JC, Georgi N, Wu L, van Blitterswijk CA, Karperien M. Cell sources for articular cartilage repair strategies: shifting from monocultures to cocultures. Tissue Eng Part B Rev 2013;19(1):31–40.
[25] Jurgens WJ, Kroeze RJ, Zandieh-Doulabi B, van Dijk A, Renders GA, Smit TH, van Milligen FJ, Ritt MJ, Helder MN. One-step surgical procedure for the treatment of osteochondral defects with adipose-derived stem cells in a caprine knee defect: a pilot study. Biores Open Access 2013;2(4):315–25.
[26] Ando W, Tateishi K, Hart DA, Katakai D, Tanaka Y, Nakata K, Hashimoto J, Fujie H, Shino K, Yoshikawa H, Nakamura N. Cartilage repair using an in vitro generated scaffold-free tissue-engineered construct derived from porcine synovial mesenchymal stem cells. Biomaterials 2007;28(36):5462–70.
[27] Fu WL, Zhou CY, Yu JK. A new source of mesenchymal stem cells for articular cartilage repair: mSCs derived from mobilized peripheral blood share similar biological characteristics in vitro and chondrogenesis in vivo as MSCs from bone marrow in a rabbit model. Am J Sports Med 2014;42(3):592–601.
[28] Mesallati T, Buckley CT, Kelly DJ. Engineering articular cartilage-like grafts by self-assembly of infrapatellar fat pad-derived stem cells. Biotechnol Bioeng 2014;111(8):1686–98.
[29] Mesallati T, Sheehy EJ, Vinardell T, Buckley CT, Kelly DJ. Tissue engineering scaled-up, anatomically shaped osteochondral constructs for joint resurfacing. Eur. Cell Mater. 2015;30:185–6. 163-85.
[30] Hubka KM, Dahlin RL, Meretoja VV, Kasper FK, Mikos AG. Enhancing chondrogenic phenotype for cartilage tissue engineering: monoculture and coculture of articular chondrocytes and mesenchymal stem cells. Tissue Eng Part B Rev 2014;20(6):641–54.
[31] Meretoja VV, Dahlin RL, Kasper FK, Mikos AG. Enhanced chondrogenesis in co–cultures with articular chondrocytes and mesenchymal stem cells. Biomaterials 2012;33(27):6362–9.
[32] Bian L, Zhai DY, Mauck RL, Burdick JA. Coculture of human mesenchymal stem cells and articular chondrocytes reduces hypertrophy and enhances functional properties of engineered cartilage. Tissue Eng Part A 2011;17(7–8):1137–45.
[33] Almeida HV, Cunniffe GM, Vinardell T, Buckley CT, O'Brien FJ, Kelly DJ. Coupling freshly isolated CD44(+) infrapatellar fat pad-derived stromal cells with a TGF-beta3 eluting cartilage ECM-derived scaffold as a single-stage strategy for promoting chondrogenesis. Adv Healthc Mater 2015;4(7):1043–53.
[34] Levingstone TJ, Moran C, Almeida HV, Kelly DJ, O'Brien FJ. Layer-specific stem cell differentiation in tri-layered tissue engineering biomaterials: towards development

of a single-stage cell-based approach for osteochondral defect repair. Mater Today Bio 2021;12:100173.
[35] Gleeson JP, Plunkett NA, O'Brien FJ. Addition of hydroxyapatite improves stiffness, interconnectivity and osteogenic potential of a highly porous collagen-based scaffold for bone tissue regeneration. Eur Cell Mater 2010;20:218–30.
[36] Haugh MG, Murphy CM, McKiernan RC, Altenbuchner C, O'Brien FJ. Crosslinking and mechanical properties significantly influence cell attachment, proliferation, and migration within collagen glycosaminoglycan scaffolds. Tissue Eng Part A 2011;17(9–10):1201–8.
[37] Koh JL, Wirsing K, Lautenschlager E, Zhang LO. The effect of graft height mismatch on contact pressure following osteochondral grafting: a biomechanical study. Am J Sports Med 2004;32(2):317–20.
[38] Giannini S, Mazzotti A, Vannini F. Bipolar fresh total osteochondral allograft in the ankle: is it a successful long-term solution? Injury 2017.
[39] Tschon M, Veronesi F, Giannini S, Fini M. Fresh osteochondral allotransplants: outcomes, failures and future developments. Injury 2017.
[40] Almeida HV, Liu Y, Cunniffe GM, Mulhall KJ, Matsiko A, Buckley CT, O'Brien FJ, Kelly DJ. Controlled release of transforming growth factor-beta3 from cartilage-extra-cellular-matrix-derived scaffolds to promote chondrogenesis of human-joint-tissue-derived stem cells. Acta Biomater 2014;10(10):4400–9.
[41] Ahearne M, Liu Y, Kelly DJ. Combining freshly isolated chondroprogenitor cells from the infrapatellar fat pad with a growth factor delivery hydrogel as a putative single stage therapy for articular cartilage repair. Tissue Eng Part A 2014;20(5–6):930–9.
[42] Mesallati T, Buckley CT, Kelly DJ. Engineering cartilaginous grafts using chondrocyte-laden hydrogels supported by a superficial layer of stem cells. J Tissue Eng Regen Med 2017;11(5):1343–53.
[43] Kamisan N, Naveen SV, Ahmad RE, Tunku K. Chondrocyte density, proteoglycan content and gene expressions from native cartilage are species specific and not dependent on cartilage thickness: a comparative analysis between rat, rabbit and goat. BMC Vet Res 2013;9(1):62.
[44] Stockwell RA. The interrelationship of cell density and cartilage thickness in mammalian articular cartilage. J Anat 1971;109(Pt 3):411–21.
[45] Cunniffe GM, Diaz-Payno PJ, Sheehy EJ, Critchley SE, Almeida HV, Pitacco P, Carroll SF, Mahon OR, Dunne A, Levingstone TJ, Moran CJ, Brady RT, O'Brien FJ, Brama PAJ, Kelly DJ. Tissue-specific extracellular matrix scaffolds for the regeneration of spatially complex musculoskeletal tissues. Biomaterials 2019;188:63–73.
[46] Schneider CA, Rasband WS, Eliceiri KW. NIH Image to ImageJ: 25 years of image analysis. Nat Methods 2012;9(7):671–5.
[47] Mainil-Varlet P, Van Damme B, Nesic D, Knutsen G, Kandel R, Roberts S. A new histology scoring system for the assessment of the quality of human cartilage repair: ICRS II. Am J Sports Med 2010;38(5):880–90.
[48] Theodoridis K, Manthou ME, Aggelidou E, Kritis A. In vivo cartilage regeneration with cell-seeded natural biomaterial scaffold implants: 15-year study. Tissue Eng Part B Rev 2021.
[49] DiBartola AC, Everhart JS, Magnussen RA, Carey JL, Brophy RH, Schmitt LC, Flanigan DC. Correlation between histological outcome and surgical cartilage repair technique in the knee: a meta-analysis. Knee 2016;23(3):344–9.
[50] Toole BP. Hyaluronan in morphogenesis. J Intern Med 1997;242(1):35–40.
[51] Sheehy EJ, Kelly DJ, O'Brien FJ. Biomaterial-based endochondral bone regeneration: a shift from traditional tissue engineering paradigms to developmentally inspired strategies. Mater Today Bio 2019;3:100009.
[52] Kronenberg HM. Developmental regulation of the growth plate. Nature 2003;423(6937):332–6.
[53] Scotti C, Tonnarelli B, Papadimitropoulos A, Scherberich A, Schaeren S, Schauerte A, Lopez-Rios J, Zeller R, Barbero A, Martin I. Recapitulation of endochondral bone formation using human adult mesenchymal stem cells as a paradigm for developmental engineering. Proc Natl Acad Sci U S A 2010;107(16):7251–6.
[54] Pallante-Kichura AL, Cory E, Bugbee WD, Sah RL. Bone cysts after osteochondral allograft repair of cartilage defects in goats suggest abnormal interaction between subchondral bone and overlying synovial joint tissues. Bone 2013;57(1):259–68.
[55] Moran CJ, Ramesh A, Brama PA, O'Byrne JM, O'Brien FJ, Levingstone TJ. The benefits and limitations of animal models for translational research in cartilage repair. J Exp Orthop 2016;3(1):1.
[56] Knutsen G, Drogset JO, Engebretsen L, Grontvedt T, Isaksen V, Ludvigsen TC, Roberts S, Solheim E, Strand T, Johansen O. A randomized trial comparing autologous chondrocyte implantation with microfracture. Findings at five years. J Bone Joint Surg Am 2007;89(10):2105–12.
[57] Basad E, Ishaque B, Bachmann G, Sturz H, Steinmeyer J. Matrix-induced autologous chondrocyte implantation versus microfracture in the treatment of cartilage defects of the knee: a 2-year randomised study. Knee Surg Sports Traumatol Arthrosc 2010;18(4):519–27.
[58] Han Y, Li H, Zhou R, Wu J, Liu Z, Wang H, Shao J, Chen Y, Zhu J, Fu Q, Qian Q, Zhou Y. Comparison between intra-articular injection of infrapatellar fat pad (IPFP) cell concentrates and IPFP-mesenchymal stem cells (MSCs) for cartilage defect repair of the knee joint in rabbits. Stem Cells Int 2021;2021:9966966.
[59] Toghraie FS, Chenari N, Gholipour MA, Faghih Z, Torabinejad S, Dehghani S, Ghaderi A. Treatment of osteoarthritis with infrapatellar fat pad derived mesenchymal stem cells in Rabbit. Knee 2011;18(2):71–5.